*Mineralogical Magazine, December 2006, Vol. 70(6), pp. 697–707*

# Influence of grinding on graphite crystallinity from experimental and natural data: implications for graphite thermometry and sample preparation

E. Crespo, F. J. Luque*, J. F. Barrenechea and M. Rodas

Departamento de Cristalografía y Mineralogía, Facultad de Geología, Universidad Complutense de Madrid, 28040 Madrid, Spain

**ABSTRACT**

This paper examines the effects of shear stress on the structural parameters that define the 'crystallinity' of graphite. The results show that highly crystalline graphite samples ground for up to 120 min do not undergo detectable changes in the three-dimensional arrangement of carbon layers but crystallite sizes ($L_c$ and $L_a$) decrease consistently with increasing grinding time. Grinding also involves particle-size diminution that results in lower temperatures for the beginning of combustion and exothermic maxima in the differential thermal analysis curves. These changes in the structural and thermal characteristics of graphite upon grinding must be taken into account when such data are used for geothermometric estimations.

Tectonic shear stress also induces reduction of the particle size and the $L_c$ and $L_a$ values of highly crystalline graphite. Thus, the temperature of formation of graphite according to structural as well as thermal data is underestimated by up to 100ºC in samples that underwent the most intense shear stress. Therefore, application of graphite geothermometry to fluid-deposited veins where graphite is the only mineral found should take into consideration the effect of tectonic shearing, or the estimated temperatures must be considered as minimum temperatures of formation only.

**Keywords:** graphite, shear stress, grinding, crystallinity, geothermometry.

## Introduction

The interpretation of the origin of graphite deposits is based on detailed mineralogical (mainly structural and thermal) and geochemical (mainly stable carbon isotope ratios) data. Studies dealing with the structural characterization of graphite are focused on the degree of continuity of the layers of carbon atoms in the structure. The degree of crystalline perfection up to the point of obtaining the ideal graphite structure is usually defined as 'crystallinity'. Graphite 'crystallinity' can be described both along the stacking direction (*c* axis) of the carbon layers and along the *a*-*b* plane. In the first case, highly crystalline graphite has shorter spacing between adjacent layers of carbon atoms (the $d_{002}$ spacing from which the *c* parameter is calculated). In addition, the continuity of the carbon layers along the stacking direction (the $L_c$ crystallite size) is larger than for poorly crystalline graphite. In the second case, 'crystallinity' refers to the continuity of carbon layers along the in-plane directions (defined by the $L_a$ crystallite size). In natural environments, 'crystallinity' has been proved to increase (smaller $d_{002}$, larger $L_c$ and $L_a$) with increasing metamorphic grade (Landis, 1971; Grew, 1974; Diessel *et al*., 1978; Kwiecinska, 1980; Buseck and Bo-Jun, 1985; Pasteris and Wopenka, 1991; Wopenka and Pasteris, 1993; Wada *et al.*, 1994; Yui *et al.*, 1996; Nishimura *et al.*, 2000; Beyssac *et al.*, 2002*b*, 2004). In particular, at low-grade metamorphic conditions it has been shown that shear stress enhances the 'crystallinity' of graphitized carbonaceous matter compared with

* E-mail: jluque@geo.ucm.es
DOI: 10.1180/0026461067060358

equivalent materials under hydrostatic pressures (Barrenechea *et al.*, 1992; Suchy *et al.*, 1997; Barzoi and Guy, 2002). Experimental studies on the effects of shearing on the graphitization of carbonaceous materials point to similar conclusions (Ross and Bustin, 1990; Bustin *et al.*, 1995*a*,*b*; Beyssac *et al.*, 2003*a*).

There are, however, few data about how shear stress affects the structural characteristics of the mineral once fully crystalline graphite is formed. It must be noted that graphite has a layered structure and that changes in structural and thermal characteristics of other minerals with layered structures, mainly phyllosilicates, upon both experimental and tectonic shearing have been reported (Pérez-Rodríguez *et al.*, 1988; Fernández-Caliani and Galán, 1992; Sánchez-Soto *et al.*, 2000; Stepkowska *et al.*, 2001; Árkai *et al.*, 2002; Abad *et al.*, 2003). Previous experimental studies have shown that polishing or grinding for long periods of time may cause changes in some structural properties of graphite when monitored by Raman spectroscopy or X-ray diffraction (XRD) techniques (Nakamizo *et al.*, 1978; Pasteris, 1989; Salver-Disma *et al.*, 1999*a*,*b*; Wakayama *et al.*, 1999; Ong and Yang, 2000). However, no comparisons between experimental data and structural changes in natural environments have been reported.

The aim of this paper is two-fold: firstly, it is intended to report the structural changes in graphite after grinding for periods usually employed in the preparation of geological samples; secondly, these results will be compared with structural data of crystalline graphite that subsequently underwent tectonic shearing as the main geological mechanism responsible for its accumulation. Both issues are important because the temperature dependence of the degree of structural ordering of graphite has been used as a geothermometer. Thus, graphite geothermometry requires that experimental and geological factors influencing changes in the graphite structure are constrained in order to obtain reliable structural data.

## Materials and methods

This experimental study on the changes of the structural characteristics of graphite upon grinding was carried out on a hand specimen from the Bogala deposit in Sri Lanka. This material is usually considered as a standard for highly crystalline graphite (Pasteris and Wopenka, 1991; Wopenka and Pasteris, 1993; Luque *et al.*, 1998). Graphite deposits from Sri Lanka were formed at granulite-facies conditions and temperatures of 750–800ºC (Katz, 1987; Dissanayake, 1994).

Small, optically homogeneous, portions (0.3–0.5 g) of the sample were crushed and ground in two different experimental devices. The first one was an agate mortar (Reitsch RMO) in which the shear stress is applied normal to the surface of the mineral grains. The second one was an X-wing mill (Culatti MFC CZ13), in which the stress is applied parallel to the surface of the grain. This mill is specially designed for platy minerals and favours delamination without mechanical disruption of the continuity of the layered structure. In both cases, graphite samples were ground for 1, 3, 5, 10, 30, 60 and 120 min. Five samples for each grinding period were prepared in order to check the precision of the results. The ground samples were then sieved through a 53 μm mesh.

The effect of tectonic shearing on graphite was studied on samples from a vein-shaped occurrence that is found along the contact between a hydrothermal quartz vein and a graphite-bearing quartzite layer. The geological, mineralogical and isotopic evidence support its formation by physical remobilization of graphite from the quartzite (Crespo *et al.*, 2005) that appears to have operated along distances of up to several metres and formed monomineralic graphite aggregates. Thus, for graphite in the vein, the greater the distance to the quartzite the greater the tectonic shear stress. Samples were collected from the graphite-bearing quartzite and from the vein-shaped graphite concentration at different distances from the contact with the quartzite (Table 1). These samples were ground for 1 min in the agate mortar.

The structural study of graphite was performed by powder XRD, Raman spectroscopy and high-resolution transmission electron microscopy (HRTEM). The XRD patterns were obtained in a Siemens Kristalloflex 810 diffractometer, using Cu-$K\alpha$ radiation at 40 kV and 30 mA, a step size of 0.03º2θ, and time per step of 1 s. Each sample was run at least twice using silicon as the internal standard. Measurements on the XRD patterns were done using the *Diffract AT* software. The Raman spectroscopy study was carried out with a DILOR XY Raman Spectrometer attached to an Olympus metallographic microscope. The excitation was done using an $Ar^+$ laser beam focused

TABLE 1. Data for graphite samples from the vein-shaped graphite and adjacent quartzite occurrences. $L_c$ crystallite size calculated after Wada *et al*. (1994): $L_c = K\lambda/FWHM_{002}\cos\theta$, where K = 0.9, λ = radiation wavelength, $FWHM_{002}$ = full-width at half-height of the 002 peak (in radians), and θ = diffraction angle at peak maximum. $L_a$ crystallite size calculated after the graph of Wopenka and Pasteris (1993).

| Sample | | H-2 | H-5 | H-13 | H-10 |
|---|---|---|---|---|---|
| Location | | Quartzite | Vein | Vein | Vein |
| Distance to the contact (m) | | – | 0.05 | 0.5 | 1.5 |
| Lustre | | Metallic | Metallic | Metallic | Dusty |
| Grain size (μm) | | 100 | 50 | 50 | 25 |
| X-ray diffraction | $d_{002}$ (Å) | 3.354 | 3.356 | 3.356 | 3.358 |
| | $FWHM_{002}$ (Δº2θ) | 0.225 | 0.236 | 0.242 | 0.270 |
| | $L_c$ (Å) | 466 | 439 | 386 | 384 |
| Raman | $I_D/I_O$ | 0 | 0.01 | 0.04 | 0.05 |
| | $A_D/(A_D+A_O)$ area ratio | 0 | 0.003 | 0.110 | 0.140 |
| | $L_a$ (Å) | >2000 | >2000 | 760 | 490 |
| DTA | $T_{max}$ (ºC) | 772 | 766 | n.d. | 673 |
| | $T_{ini}$ (ºC) | 610 | 589 | n.d. | 540 |

n.d. not determined

through the microscope objective. The measurements were done under the usual experimental conditions (λ = 514.5 nm, 100 × objective, nA = 0.95), with a nominal spatial resolution of ~1 μm and a spectral resolution of ~1 $cm^{-1}$. The first-order Raman spectra were recorded from 900 to 1800 $cm^{-1}$. The second order spectra were recorded from 2400 to 3100 $cm^{-1}$. The position, height, width (FWHM), and area of the disorder peak (*D*, at ~1360 $cm^{-1}$) and order peak (O, at ~1582 $cm^{-1}$) in the first-order Raman spectra were measured. The software used was *Labspec* v. 2.08. Five runs of each sample were recorded to check the precision of the data.

The HRTEM images were obtained at the 'Centro de Microscopía Luis Bru' of the Universidad Complutense with a JEOL JEM-4000 EX electron microscope operated at 400 kV. Samples were dispersed in acetone and then deposited onto TEM grids previously coated with a holey-carbon film.

A complementary thermal study was carried out because the temperature of combustion of carbon in graphite is related to its temperature of formation and it is therefore linked to graphite 'crystallinity' (Kwiecinska, 1980; Cebulak *et al.*, 1999*a*,*b*). Differential thermal analysis (DTA) curves were recorded by heating the sample at 10ºC/min in the range 20 to 1000ºC with a continuous air supply of 50 ml/min in a Seiko TG/DTA 320U apparatus. Alumina was used as the reference material.

## Results

### *Powder XRD*

All of the XRD patterns of ground graphite correspond to highly crystalline hexagonal graphite. No peaks of rhombohedral graphite were recorded. Increasing grinding time affects the values of the structural parameters determined from the XRD patterns in different ways (Table 2). The measured $d_{002}$ spacing shows no significant variation with increasing grinding time, whatever the grinding device. However, the measured full-width at medium height of the 002 peak ($FWHM_{002}$) is more sensitive to the type and duration of grinding. The $FWHM_{002}$ values clearly increase for grinding times of >60 min in the agate mortar and involve a reduction of 50–110 Å in the calculated crystallite size along the *c* axis ($L_c$) compared with the samples ground for 1 to 30 min. Samples ground in the X-wing mill show no significant changes in the $FWHM_{002}$, and $L_c$ values plot in a tight cluster in the range between 400 and 450 Å (Fig. 1).

TABLE 2. Structural data (XRD and Raman) of the graphite samples ground experimentally. Numbers in parentheses correspond to the standard deviation. $L_c$ crystallite size calculated after Wada *et al*. (1994). $L_a$ crystallite size calculated after Wopenka and Pasteris (1993).

| Grinding time (min) | XRD $d_{002}$ (Å) | XRD FWHM$_{002}$ ($\Delta 2^o\theta$) | XRD $L_c$ (Å) | Raman FWHM$_O$ ($cm^{-1}$) | Raman $I_D/I_O$ | Raman $A_D/(A_D+A_O)$x100 area ratio | Raman $L_a$ (Å) |
|---|---|---|---|---|---|---|---|
| Agate mortar | | | | | | | |
| 1 | 3.357 (0.002) | 0.22 (0.02) | 464 (50) | 16 (4) | 0.14 (0.03) | 1 (1) | >2000 |
| 3 | 3.358 (0.002) | 0.22 (0.01) | 468 (24) | 21 (4) | 0.17 (0.06) | 4 (3) | >2000 |
| 5 | 3.356 (0.002) | 0.21 (0.01) | 483 (29) | 19 (2) | 0.16 (0.02) | 4 (2) | >2000 |
| 10 | 3.356 (0.001) | 0.22 (0.01) | 470 (19) | 20 (2) | 0.16 (0.03) | 5 (3) | >2000 |
| 30 | 3.357 (0.001) | 0.23 (0.01) | 446 (14) | 19 (3) | 0.17 (0.05) | 9 (6) | 1300 |
| 60 | 3.357 (0.012) | 0.26 (0.01) | 395 (19) | 19 (2) | 0.12 (0.01) | 3 (2) | >2000 |
| 120 | 3.355 (0.003) | 0.28 (0.01) | 373 (11) | 23 (4) | 0.20 (0.05) | 11 (4) | 900 |
| X-wing mill | | | | | | | |
| 1 | 3.356 (0.002) | 0.24 (0.01) | 428 (23) | 16 (4) | 0.11 (0.01) | 3 (1) | >2000 |
| 3 | 3.355 (0.004) | 0.25 (0.01) | 423 (12) | 19 (3) | 0.12 (0.02) | 1 (1) | >2000 |
| 5 | 3.357 (0.004) | 0.26 (0.01) | 391 (15) | 18 (2) | 0.12 (0) | 1 (0) | >2000 |
| 10 | 3.353 (0.002) | 0.24 (0.01) | 448 (11) | 20 (4) | 0.14 (0) | 4 (0) | >2000 |
| 30 | 3.356 (0.004) | 0.25 (0.02) | 412 (28) | 18 (1) | 0.13 (0.06) | 4 (2) | >2000 |
| 60 | 3.355 (0.003) | 0.24 (0.01) | 441 (25) | 18 (3) | 0.16 (0.04) | 6 (4) | >2000 |
| 120 | 3.355 (0.002) | 0.24 (0.01) | 441 (21) | 20 (4) | 0.15 (0.02) | 6 (4) | >2000 |

Similar relations can be observed in the tectonically sheared samples. Structural data of graphite from the quartzite correspond to well crystalline hexagonal graphite (Table 2). However, graphite in the vein-shaped occurrence shows decreasing 'crystallinity' with increasing distance from the quartzite. The variation in the 002 spacing is slight but the FWHM$_{002}$ increases consistently with increasing distance from the contact. Conversely, the $L_c$ values decrease in those samples collected at greater distances from the contact with the graphite-bearing quartzite.

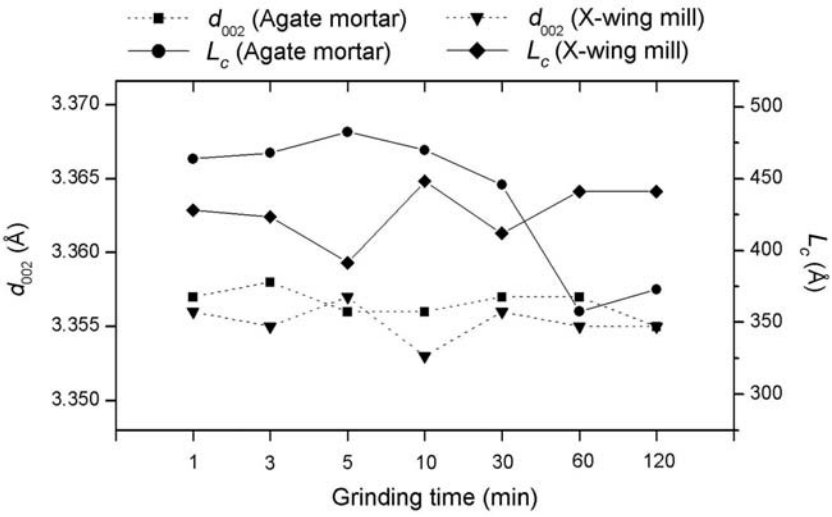


FIG. 1. Variation of $d_{002}$ and crystallite size $L_c$ of Sri Lankan graphite with grinding time for each grinding device.

### *Raman spectroscopy*

The Raman spectra of experimentally ground samples are typical of highly crystalline graphite. The first-order Raman spectra are characterized by sharp and symmetrical O peaks and no or very weak D peaks. The FWHM values of the O peaks do not vary (within error) for either grinding device and are similar for both mills. In spite of the fact that the 60 min data for the agate mortar look anomalous, the intensity and area of the D peak show a slight but progressive increase with increasing grinding time in both experimental devices (Table 2). This results in greater $A_D/(A_D+A_O)$ ratios and hence in smaller crystallite size along the basal plane ($L_a$). The second-order Raman spectra do not show any variation related to the grinding device or duration of grinding. These spectra only display sharp and narrow $S_2$ peaks with a shoulder at ~2690 $cm^{-1}$. The features of the second-order Raman spectra are therefore typical of highly crystalline graphite (Lespade *et al.*, 1982; Pasteris and Wopenka, 1991; Wopenka and Pasteris, 1993).

Some interesting variations are recorded in the Raman spectra of graphite from the natural occurrence in which solid-state remobilization operated. First-order Raman spectra of graphite from the quartzite do not display the D peak (Fig. 2), thus indicating its high 'crystallinity' along the basal plane. Graphite in the vein-shaped occurrence shows progressively better defined D peaks with increasing distance from the contact with the quartzite layer (Fig. 2). The intensity and area ratios of the D to O peaks also increase with increasing distance from the contact (Table 1). The continuity of the layers along the basal plane ($L_a$) therefore experiences a significant decrease from >2000 Å to some 500 Å. The second-order Raman spectra do not record any significant change in the graphite samples from the vein-shaped occurrence with respect to those from the quartzite. The features of the second-order Raman spectra include well defined $S_2$ peaks and a shoulder at ~2685 $cm^{-1}$ that correspond to highly crystalline graphite (Fig. 2). The disorder band ($S_3$) at ~2950 $cm^{-1}$ was not recorded in the second-order Raman spectra.

### *HRTEM*

The study by HRTEM was performed on three samples of experimentally ground graphite selected after XRD and Raman data. Samples selected for this study were those in which major changes in the 'crystallinity' with increasing grinding times were observed: 30 min in the agate mortar, 120 min in the agate mortar and 120 min in the X-wing mill.

After grinding for 30 min in the agate mortar, lattice-fringe images show that the layers of carbon atoms are still parallel, but the surface of the particles became corrugated (Fig. 3*a*). After 120 min, graphite particles show a large number of carbon layers stacked coherently, but corrugation of the layers is evident at the edge of the particles (Fig. 3*b*). These corrugated layers evolve to small tangle-like domains (Fig. 3*c*). The continuity of the layers along the stacking direction in these domains is significantly less (<10 nm).

The effect of grinding in the X-wing mill on the microtexture of the graphite particles is less

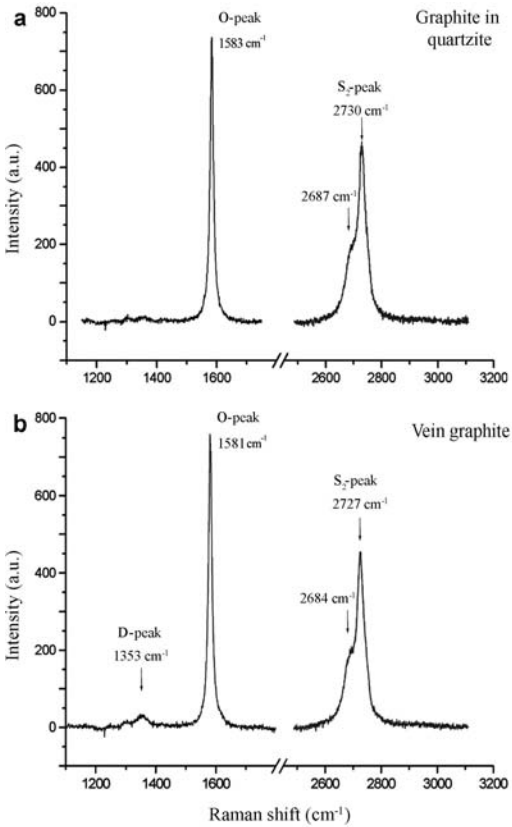


FIG. 2. First- and second-order Raman spectra of graphite samples from (*a*) graphite-bearing quartzite, and (*b*) vein-shaped occurrence (sample H-13). Note the development of the disorder peak ($D_1$) in the first-order Raman spectrum of the graphite sample from the vein as the result of tectonic shearing.

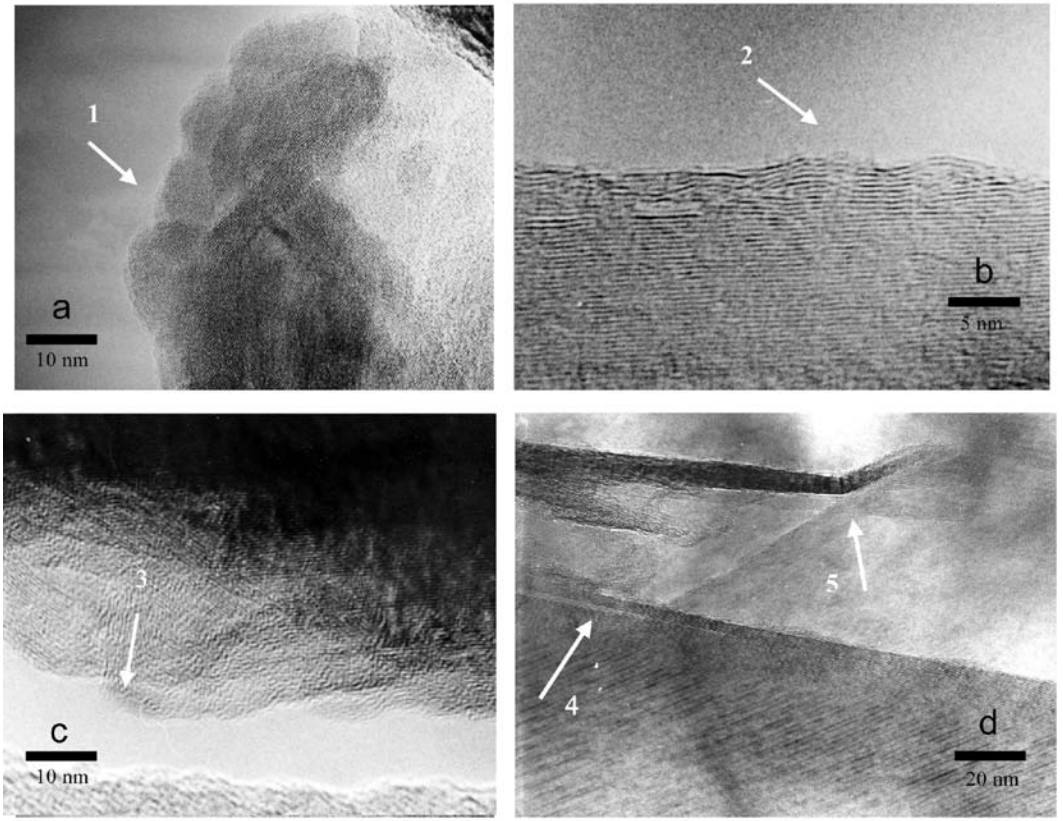


FIG. 3. HRTEM lattice-fringe images of experimentally ground Sri Lankan graphite. (*a*) Turbostratic-like arrangement of carbon layers at the edges of graphite particles (point 1). Sample ground for 30 min in an agate mortar. (*b*) Parallel arrangement of carbon layers showing displacements and corrugation of the layers at the edge of the particle (point 2). Sample ground for 120 min in an agate mortar. (*c*) Detail of the tangle-like domains (point 3) in the graphite particles of the sample ground for 120 min in an agate mortar. (*d*) Delamination of the graphite particles along the basal plane with preservation of the crystallite size $L_a$ (point 4) and bending of the layers (point 5). Sample ground for 120 min in the X-wing mill.

pronounced. After 120 min, the graphite particles are separated into thinner flakes as a result of delamination. The continuity of the carbon layers along the basal plane in these flakes is preserved (Fig. 3*d*). In some cases, the layers can be folded but in contrast with the tangle-like domains observed in the sample ground in the agate mortar there is no evidence of disruption in the surface of the particles.

### *DTA*

The DTA curves of the experimentally ground graphite samples show a well defined exothermic peak at temperatures close to 800ºC for grinding times in the range of 1 to 10 min. There are no significant differences in this range for the DTA curves of graphite ground in either experimental device (Table 2). For grinding times >10 min in the agate mortar, the temperature of the exothermic maximum ($T_{max}$) shows a decrease of up to 50ºC for the samples ground for 60 and 120 min (Fig. 4*a*). In addition, the temperature at which combustion of these samples commences ($T_{ini}$) also decreases by up to 100ºC (for the sample ground for 120 min). Samples ground in the X-wing mill for >10 min also show the same trend but the decrease in temperature is smaller (up to 30ºC for the sample ground for 120 min).

A complementary study carried out on different size fractions obtained from the sample ground for 10 min in the agate mortar demonstrated the

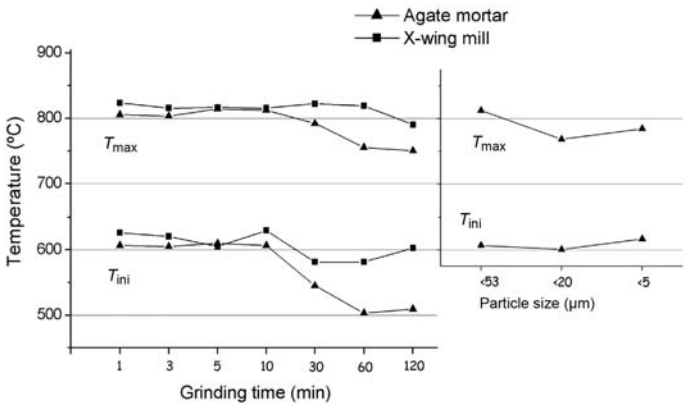


FIG. 4. (*a*) Variation of the temperature of the beginning of combustion of graphite ($T_{ini}$) and of the exothermic maximum ($T_{max}$) with grinding time for both grinding devices. (*b*) Variation of $T_{ini}$ and $T_{max}$ with particle size for the sample ground in the agate mortar for 10 min.

influence of the particle size on the DTA curve of graphite. As shown in Fig. 4*b*, $T_{ini}$ and $T_{max}$ decrease in the <20 µm fraction compared with the <53 µm fraction. In turn, both temperatures increase (by up to 20ºC) for the smallest size fraction (<5 µm).

The DTA curve of graphite from the quartzite is consistent with its high crystallinity. The temperature at which combustion commences is 610ºC and the exothermic peak maximum is at 770ºC. However, in the vein-shaped occurrence, dusty graphite from the sample located at the greatest distance from the contact with the quartzite has the smallest exothermic peak maximum (673ºC). In addition, the temperature at which combustion commences ($T_{ini}$ = 540ºC) is also the smallest recorded for the set of samples collected from the vein-shaped occurrence.

## Discussion

The results obtained from this study clearly point to the influence of shear stress on the structural and thermal properties of graphite. The overall experimental data indicate that increasing shear stress (longer grinding times) involves a reduction in the 'crystallinity', both along the stacking direction of the carbon layers and along the basal plane in the graphite structure (Table 2). Structural and thermal data for graphite from the vein-shaped occurrence in which physical remobilization in the solid state by tectonic shear stress operated as the main mechanism for graphite accumulation also show a similar trend (Table 1).

The results of this study are in accordance with previous data obtained after prolonged grinding on laboratory-prepared graphite (Salver-Disma *et al.*, 1999*a*,*b*). In contrast to these previous studies, we present here experimental data for grinding times usually employed for geological samples. The results also indicate that the type of mechanical milling affects with different intensity the changes in graphite 'crystallinity'. These considerations must be borne in mind during the preparation of graphite-bearing rock samples since some structural parameters of graphite have been used as potential geothermometers (Shengelia *et al.*, 1979; Rietmeijer and Mackinnon, 1985; Luque *et al.*, 1993; Wada *et al.*, 1994; Malisa, 1998; Beyssac *et al.*, 2002*a*; Rahl *et al.*, 2005).

Overall, the structural data of experimentally ground samples show that shear stress applied normal to the surface of the graphite grains (agate mortar) induces greater changes in 'crystallinity' than samples delaminated using shear stress parallel to the surface of the particles (X-wing mill). For the shorter grinding periods tested (<30 min) there is no significant change in the XRD patterns of graphite irrespective of the grinding device, suggesting that the graphite structure remains unaffected. Samples ground for >30 min in the agate mortar display a noticeable decrease in the $L_c$ values which correlates with the most important changes in the intensity and area ratios of the O and D peaks recorded in the first-order Raman spectra (Table 2). This trend has been proved to continue for longer grinding

periods (from 4 to 200 h) in natural graphite (Nakamizo *et al.*, 1978), although such long grinding times are not realistic for any graphite-bearing rock. As revealed by the HRTEM images, for the grinding times used in our study, the formation of small tangle-like domains (with limited continuity of the layers of carbon atoms both along the stacking direction and the *a-b* plane) occurs. However, these microtextural changes do not affect the three-fold arrangement of carbon atoms in the structure because the $S_1$ band (with peak splitting at 2690 and 2735 $cm^{-1}$) is still well defined in the second-order Raman spectra (Lespade *et al.*, 1982). Thus, the increase in the $FWHM_{002}$ in the XRD patterns and the increase in the $I_D/I_O$ and $A_D/(A_D+A_O)$ ratios in the Raman spectra reflect the mechanical disruption of the original graphite particles that leads to smaller grain and crystallite sizes (Klug and Alexander, 1974; Lespade *et al.*, 1982; Salver-Disma *et al.*, 1999*b*). The formation of graphite particles with smaller grain and crystallite sizes under shear stresses is due to the weak interlayer bonding in the graphite structure. Salver-Disma *et al.* (1999*b*) reported that prolonged grinding (>20 h) breaks the in-plane covalent bonds of carbon atoms in the graphite structure resulting in larger $d_{002}$ spacings. In addition, Nakamizo *et al.* (1978) showed that the rhombohedral polytype of graphite can be formed after grinding natural hexagonal graphite for >30 h.

Therefore, using experimental periods commonly employed in the preparation of geological samples (<10 min), the graphite structure is not significantly disturbed and the greatest variation in the $d_{002}$ value results in a difference of <50ºC in the geothermometric estimation graph of Shengelia *et al.* (1979) that relates the *c* parameter of graphite with the temperature of formation. On the other hand, for a grinding period of 120 min in the agate mortar, there is an important change in the $A_D/(A_D+A_O)$ ratio and hence in the temperature of formation estimated according to the geothermometer of Beyssac *et al.* (2002*a*). Unfortunately, this geothermometer is defined for temperatures up to ~650ºC. If we consider that the graphite from Sri Lanka used in this experimental study was formed under granulite-facies conditions at temperatures close to 750–800ºC (e.g. Katz, 1987), then the largest $A_D/(A_D+A_O)$ ratios (~0.11) would lead to an underestimation of the temperature of graphite formation of ~150–200ºC. These results reveal a loss of 'crystallinity' at the Raman scale upon grinding and are in agreement with those previously reported by Pasteris (1989) and Beyssac *et al.* (2003*b*) on the effects of polishing for the *in situ* study of graphite-bearing rock samples in thin section.

Concerning the thermal study, $T_{ini}$ and $T_{max}$ show a noticeable decrease in grinding times >10 min in the agate mortar. Previous experimental work on both synthetic and natural graphite indicates that the surface area increases with increasing grinding time (Nakamizo *et al.*, 1978; Salver-Disma *et al.*, 1999*a*,*b*; Wakayama *et al.*, 1999). This increase in the surface area of the ground samples is responsible for the ease with which oxygen in air is chemisorbed onto graphite (Nakamizo *et al.*, 1978). Thus, the reduction of grain size upon grinding causes the observed decrease in both $T_{ini}$ and $T_{max}$ in the DTA curves since these analyses were performed with a continuous air supply to the sample. Such an interpretation is supported by the results of the complementary study on the relationship between the grain size of the graphite particles and the characteristics of the DTA curves (Fig. 4*b*). Very small particle sizes (<5 μm in this study), however, drive $T_{ini}$ and $T_{max}$ in the opposite direction. Residual electrostatic forces among graphite particles may cause them to agglomerate, leading to larger effective grain sizes. Therefore, $T_{ini}$ and $T_{max}$ are displaced to slightly higher values. The aggregation of graphite particles can be correlated with the decrease in the surface area after intensive grinding of synthetic graphite reported by Salver-Disma *et al.* (1999*a*,*b*) and Wakayama *et al.* (1999).

Tectonic shearing on highly crystalline graphite operates in the same way as experimental grinding does. Graphite in the quartzite occurs as disseminated flakes with sizes of ~100 μm. The vein-shaped occurrence consists of an accumulation of smaller graphite crystals (25–60 μm). The solid-state remobilization of graphite from the quartzite caused the mechanical disruption of graphite that led to the reduction in particle size of graphite crystals within the vein (Crespo *et al.*, 2005). For this, the greater the distance to the quartzite the greater the tectonic shear stress. Thus, longer distances to the contact with the quartzite resulted in an enhanced reduction of the grain size of the graphite crystals (Table 1) observed at the optical microscope. In a similar way, the crystallite sizes ($L_c$ and $L_a$) of graphite disseminated within the quartzite are consistently larger than in the vein. In turn, samples located at

progressively longer distances from the quartzite also have smaller crystallite sizes. In addition, $d_{002}$ values are slightly lower in the graphite disseminated in the quartzite ($d_{002}$ = 3.354 Å) than in the samples from the vein-shaped occurrence ($d_{002}$ = 3.356−3.358 Å). The temperature obtained from the *c* parameter of graphite in the quartzite using the geothermometric estimation of Shengelia *et al.* (1979) is 710±10ºC. This temperature is consistent with the sillimanite facies of the host rocks (Crespo *et al.*, 2005). However, the *c* parameter of graphite in the vein corresponds to lower temperatures (600−675ºC). The $A_D/(A_D+A_O)$ ratio in the Raman spectra also has a maximum value (0.14) for the sample located at the longest distance from the contact (H-10). This provides a temperature close to 600ºC using the geothermometer of Beyssac *et al.* (2002*a*), a value that is in good agreement with that obtained from the *c* parameter, but yields a difference of ~110ºC with the estimated temperature for graphite in the quartzite. The DTA results also show the effect of greater tectonic shearing on the graphite samples from the vein-shaped occurrence far away from the contact with the quartzite. Again, the sample H-10 which has the smallest grain size has the minimum values of $T_{ini}$ and $T_{max}$.

In summary, the results of the structural study reveal that tectonic shearing does not influence changes in the three-dimensional order of graphite (the $d_{002}$ values and the features of the second-order Raman spectra remain apparently unaffected). However, the parameters that reflect the continuity of carbon layers in the structure of graphite ($L_c$ and $L_a$) indicate a loss of 'crystallinity' with increasing tectonic shear stress. These changes have a noticeable effect on the temperature of formation estimated according to the different graphite geothermometers.

## Conclusions

The results of this study allow us to establish the following:

(1) Mechanical grinding for the preparation of graphite samples affects the particle size of graphite grains but causes little disruption of the structure.

(2) Experimental grinding in which shear stress is applied normal to the basal plane of graphite grains (agate mortar) has a greater effect than milling by shearing parallel to those planes (X-wing mill). The use of the X-wing mill is recommended for any study based on the structural characteristics of graphite.

(3) The disruption of the continuity of the carbon layers in the graphite structure results in smaller crystallite sizes ($L_c$ and $L_a$). The disorder band in the first-order Raman spectra grows progressively with increasing grinding times, especially for the agate mortar. Thus, geothermometric estimations based on the order- to disorder-band area ratio are affected by prolonged grinding (>30 min).

(4) Grain-size reduction during grinding results in lower temperatures for the commencement of combustion and maximum exothermic peak in the DTA curves. Therefore, previous studies by optical microscopy are needed to determine the original size of the graphite particles. Grinding below that size should be avoided.

(5) Tectonic shearing causes variations both in grain size and in the continuity of carbon layers in the structure of graphite. As observed in the vein-shaped graphite occurrence, the reduction of grain size can be correlated with the decrease of some 'crystallinity' markers (mainly $L_c$ and $L_a$). This yields an underestimation of the temperature of formation by using graphite geothermometers based on XRD or Raman spectroscopy data or on the position of the exothermic maximum in the DTA curve.

(6) The effects of experimental grinding or tectonic shearing must be considered in studies of fluid-deposited graphite veins, where graphite is commonly the only mineral found. The preservation of delicate textures such as spherulites, rosettes or aggregates of bladed graphite crystals in such deposits (Luque *et al.*, 1998) may allow us to rule out the effect of tectonic shearing, otherwise the temperature estimated using any graphite geothermometer must be considered as a minimum temperature.

## Acknowledgements

The authors thank Prof. C.B. Dissanayake for providing the graphite sample from the Bogala deposit used in the experimental study. Technical assistance by Dr R. Rojas and J.P. Boudou during the thermal and Raman spectroscopy studies is also gratefully acknowledged. The comments and suggestions of an anonymous reviewer helped to improve the manuscript. This work has been supported by Projects PB98-0836 and CGL2006-00835 of the Spanish Ministry of Education and Science.

## References


Abad, I., Gutiérrez-Alonso, G., Nieto, F., Gertner, I., Becker, A. and Cabero, A. (2003) The structure and the phyllosilicates (chemistry, crystallinity and texture) of Talas Ala-Tau (Tien Shan, Kyrgyz Republic); comparison with more recent subduction complexes. *Tectonophysics*, **365**, 103–127.

Árkai, P., Ferreiro Maehlmann, R., Suchy, V., Balogh, K., Sykorova, I. and Frey, M. (2002) Possible effects of tectonic shear strain on phyllosilicates; a case study from the Kandersteg area, Helvetic domain, Central Alps, Switzerland. *Schweizerische Mineralogische und Petrographische Mitteilungen*, **82**, 273–290.

Barrenechea, J.F., Rodas, M. and Arche, A. (1992) Relation between graphitization of organic matter and clay mineralogy, Silurian black shales in Central Spain. *Mineralogical Magazine*, **56**, 477–485.

Barzoi, S.C. and Guy, B. (2002) Role of metamorphic strain in the crystallinity of graphite: the example of the graphitic schists from the Lotru valley (Carpathians, Romania). *Comptes Rendus Geoscience*, **334**, 89–95.

Beyssac, O., Goffé, B., Chopin, C. and Rouzaud, J.-N. (2002*a*) Raman spectra of carbonaceous material in metasediments: a new geothermometer. *Journal of Metamorphic Geology*, **20**, 859–871.

Beyssac, O., Rouzaud, J.-N., Goffé, B., Brunet, F. and Chopin, C. (2002*b*) Graphitization in a high-pressure, low-temperature metamorphic gradient: a Raman microspectroscopy and HRTEM study. *Contributions to Mineralogy and Petrology*, **143**, 19–31.

Beyssac, O., Brunet, F., Petitet, J.P., Goffé, B. and Rouzaud, J.-N. (2003*a*) Experimental study of the microtextural and structural transformations of carbonaceous material under pressure and temperature. *European Journal of Mineralogy*, **15**, 937–951.

Beyssac, O., Goffé, B., Petitet, J.P., Froigneux, E., Moreau, M. and Rouzaud, J.-N. (2003*b*) On the characterization of disordered and heterogeneous carbonaceous materials by Raman spectroscopy. *Spectrochimica Acta, Part A*, **59**, 2267–2276.

Beyssac, O., Bollinger, L., Avouac, J.P. and Goffé, B. (2004) Thermal metamorphism in the Lesser Himalaya of Nepal determined from Raman spectroscopy of carbonaceous material. *Earth and Planetary Science Letters*, **225**, 233–241.

Buseck, P.R. and Bo-Jun, H. (1985) Conversion of carbonaceous material to graphite during metamorphism. *Geochimimica et Cosmochimica Acta*, **49**, 2003–2016.

Bustin, R.M., Ross, J.V. and Rouzaud, J.N. (1995*a*) Mechanisms of graphite formation from kerogen: experimental evidence. *International Journal of Coal Geology*, **28**, 1–36.

Bustin, R.M., Rouzaud, J.-N. and Ross, J.V. (1995*b*) Natural graphitization of anthracite: Experimental considerations. *Carbon*, **33**, 679–691.

Cebulak, S., Gaweda, A. and Hanak, B. (1999*a*) Dispersed organic matter as an indicator of the metamorphic processes – the example of graphites from western Tatra crystalline basament. *Acta Montanistica Slovaca*, **4**, 197–198.

Cebulak, S., Gawêda, A. and Langier-Kuźniarowa, A. (1999*b*) Oxyreactive thermal analysis of dispersed organic matter, kerogen and carbonization products. *Journal of Thermal Analysis and Calorimetry*, **56**, 917–924.

Crespo, E., Luque, F.J., Barrenechea, J.F. and Rodas, M. (2005) Mechanical graphite transport in fault zones and the formation of graphite veins. *Mineralogical Magazine*, **69**, 463–470.

Diessel, P.R., Brothers, R.N. and Black, P.M. (1978) Coalification and graphitization in high-pressure schists in New Caledonia. *Contributions to Mineralogy and Petrology*, **68**, 63–78.

Dissanayake, C.B. (1994) Origin of vein graphite in high-grade metamorphic terrains. *Mineralium Deposita*, **29**, 57–67.

Fernández-Caliani, J.C. and Galán, E. (1992) Influence of tectonic factors on illite crystallinity: a case study in the Iberian Pyrite Belt. *Clay Minerals*, **27**, 385–388.

Grew, E.S. (1974) Carbonaceous material in some metamorphic rocks of New England and other areas. Journal of *Geology*, **82**, 50–73.

Katz, M.B. (1987) Graphite deposits of Sri Lanka: a consequence of granulite facies metamorphism. *Mineralium Deposita*, **22**, 18–25.

Klug, H.P. and Alexander, L.E. (1974) *X-ray Diffraction Procedures for Polycrystalline and Amorphous Materials*, 2nd edition. John Wiley, New York.

Kwiecinska, B. (1980) Mineralogy of natural graphites. *Polska Akademii Nauk, Prace Mineralogiczne*, **67**, 5–79.

Landis, C.A. (1971) Graphitization of dispersed carbonaceous material in metamorphic rocks. *Contributions to Mineralogy and Petrology*, **30**, 34–45.

Lespade, P., Al-Jishi, R. and Dresselhaus, M.S. (1982) Model for Raman scattering from incompletely graphitized carbons. *Carbon*, **20**, 427–431.

Luque, F.J., Barrenechea, J.F. and Rodas, M. (1993) Graphite geothermometry in low and high temperature regimes: two case studies. *Geological Magazine*, **130**, 501–511.

Luque, F.J., Pasteris, J.D., Wopenka, B., Rodas, M. and Barrenechea, J.F. (1998) Natural fluid-deposited graphite: mineralogical characteristics and mechanisms of formation. *American Journal of Science*,

**298**, 471–497.

Malisa, E.P. (1998) Application of graphite as a geothermometer in hydrothermally altered metamorphic rocks of the Merelani-Lelatema area, Mozambique Belt, northeastern Tanzania. *Journal of African Earth Sciences*, **26**, 313–316.

Nakamizo, M., Honda, H. and Inagaki, M. (1978) Raman spectra of ground natural graphite. *Carbon*, **16**, 281–283.

Nishimura, Y., Coombs, D.S., Landis, C.A. and Itaya, T. (2000) Continuous metamorphic gradient documented by graphitization and K-Ar age, southeast Otago, New Zealand. *American Mineralogist*, **85**, 1625–1636.

Ong, T.S. and Yang, H. (2000) Effect of atmosphere on the mechanical milling of natural graphite. *Carbon*, **38**, 2077–2085.

Pasteris, J.D. (1989) In situ analysis in geological thin-sections by Laser Raman Microprobe Spectroscopy: a cautionary note. *Applied Spectroscopy*, **43**, 567–570.

Pasteris, J.D. and Wopenka, B. (1991) Raman spectra of graphite as indicators of degree of metamorphism. *The Canadian Mineralogist*, **29**, 1–9.

Pérez-Rodríguez, J.L., Sánchez del Villar, L. and Sánchez Soto, P.J. (1988) Effects of dry grinding on pyrophyllite. *Clay Minerals*, **23**, 399–410.

Rahl, J.M., Anderson, K.M., Brandon, M.T. and Fassoulas, C. (2005) Raman spectroscopy carbonaceous material thermometry of low-grade metamorphic rocks: Calibration and application to tectonic exhumation in Crete, Greece. *Earth and Planetary Science Letters*, **240**, 339–354.

Rietmeijer, F.J.M. and Mackinnon, I.D.R. (1985) Poorly graphitized carbon as a new cosmothermometer for primitive extraterrestrial materials. *Nature*, **315**, 733–736.

Ross, J.V. and Bustin, R.M. (1990) The role of strain energy in creep graphitization of anthracite. *Nature*, **343**, 58–60.

Salver-Disma, F., Du Pasquier, A., Tarascon, J.-M., Lassègues, J.-C. and Rouzaud, J.-N. (1999*a*) Physical characterization of carbonaceous materials prepared by mechanical grinding. *Journal of Power Sources*, **81–82**, 291–295.

Salver-Disma, F., Tarascon, J.-M., Clinard, C. and Rouzaud, J.-N. (1999*b*) Transmission electron microscopy studies on carbon materials prepared by mechanical milling. *Carbon*, **37**, 1941–1959.

Sánchez-Soto, P.J., Jiménez de Haro, M.C., Pérez Maqueda, L.A., Varona, I. and Pérez-Rodríguez, J.L. (2000) Effects of grinding on the structural changes of kaolinite powders. *Journal of the American Ceramic Society*, **83**, 1649–1657.

Shengelia, D.M., Akhvlediani, R.A. and Ketskhoveli, D.N. (1979) The graphite geothermometer. *Doklady Akademii Nauk SSSR*, **235**, 132-134.

Stepkowska, E.T., Pérez-Rodríguez, J.L., Jiménez de Haro, M.C., Sánchez-Soto, P.J. and Maqueda, C. (2001) Effects of grinding and water vapour on the particle size of kaolinite and pyrophyllite. *Clay Minerals*, **36**, 105–114.

Suchy, V., Frey, M. and Wolf, M. (1997) Vitrinite reflectance and shear-induced graphitization in orogenic belts: A case study from Kandersteg area, Helvetic Alps, Switzerland. *International Journal of Coal Geology*, **34**, 1–20.

Wada, H., Tomita, T., Matsuura, K., Iuchi, K., Ito, M. and Morikiyo, T. (1994) Graphitization of carbonaceous matter during metamorphism with references to carbonate and pelitic rocks of contact and regional metamorphisms, Japan. *Contributions to Mineralogy and Petrology*, **118**, 217–228.

Wakayama, H., Mizuno, J., Fukushima, Y., Nagano, K., Fukunaga, T. and Mizutani, U. (1999) Structural defects in mechanically ground graphite. *Carbon*, **37**, 947–952.

Wopenka, B. and Pasteris, J.D. (1993) Structural characterization of kerogens to granulite-facies graphite: Applicability of Raman microprobe spectroscopy. *American Mineralogist*, **78**, 533–557.

Yui, T.F., Huang, E. and Xu, J. (1996) Raman spectrum of carbonaceous material: a possible metamorphic grade indicator for low-grade metamorphic rocks. *Journal of Metamorphic Geology*, **14**, 115–124.

[*Manuscript received 31 April 2006: revised 23 December 2006*]